

Universality aspects of the $d = 3$ random-bond Blume-Capel model

A. Malakis¹, A. Nihat Berker^{2,3}, N. G. Fytas⁴, and T. Papakonstantinou¹

¹*Department of Physics, Section of Solid State Physics,*

University of Athens, Panepistimiopolis, GR 15784 Zografos, Athens, Greece

²*Faculty of Engineering and Natural Sciences, Sabanci University, Orhanli, Tuzla 34956, Istanbul, Turkey*

³*Department of Physics, Massachusetts Institute of Technology, Cambridge, Massachusetts 02139, U.S.A. and*

⁴*Departamento de Física Teórica I, Universidad Complutense, E-28040 Madrid, Spain*

(Dated: February 19, 2022)

The effects of bond randomness on the universality aspects of the simple cubic lattice ferromagnetic Blume-Capel model are discussed. The system is studied numerically in both its first- and second-order phase transition regimes by a comprehensive finite-size scaling analysis. We find that our data for the second-order phase transition, emerging under random bonds from the second-order regime of the pure model, are compatible with the universality class of the 3d random Ising model. Furthermore, we find evidence that, the second-order transition emerging under bond randomness from the first-order regime of the pure model, belongs to a new and distinctive universality class. The first finding reinforces the scenario of a single universality class for the 3d Ising model with the three well-known types of quenched uncorrelated disorder (bond randomness, site- and bond-dilution). The second amounts to a strong violation of universality principle of critical phenomena. For this case of the ex-first-order 3d Blume-Capel model, we find sharp differences from the critical behaviors, emerging under randomness, in the cases of the ex-first-order transitions of the corresponding weak and strong first-order transitions in the 3d three-state and four-state Potts models.

PACS numbers: 75.10.Nr, 05.50.+q, 64.60.Cn, 75.10.Hk

I. INTRODUCTION

The effect of quenched randomness on the equilibrium and dynamic properties of macroscopic systems is a subject of great theoretical and practical interest. It has been known that quenched bond randomness may or may not modify the critical exponents of second-order phase transitions, based on the Harris criterion [1, 2]. It was more recently established that quenched bond randomness always affects first-order phase transitions by conversion to second-order phase transitions, for infinitesimal randomness in $d = 2$ [3, 4] and after a threshold amount of randomness in $d > 2$ [4], as also inferred by general arguments [5]. A physically attractive description for these effects has been provided by the Cardy and Jacobsen [6] mapping between the random-field Ising model and the large q ($d = 2$) q -state Potts model and the conjectured extensions of this to higher dimensions. The first numerical verification of the Cardy-Jacobsen conjecture has been presented recently in Ref. [7]. Furthermore, this rounding effect of first-order transitions has now been rigorously established in a unified way in low dimensions ($d \leq 2$) including a large variety of types of randomness in classical and quantum spin systems [8]. These predictions [3, 4] have been confirmed by Monte Carlo (MC) simulations [9]. Moreover, renormalization-group calculations on tricritical systems have revealed that not only first-order transitions are converted to second-order transitions, but the latter are controlled by a distinctive strong-coupling fixed point [10].

Recently the present authors [11] have studied details of the above mentioned expectations for the effects of quenched bond randomness on second- and first-order

phase transitions by considering the 2d random-bond version of the Blume-Capel (BC) model. Our studies have provided strong numerical evidence, using an efficient implementation of the Wang-Landau algorithm [12], clarifying these effects in 2d systems. In particular it was shown that, the second-order phase transition, emerging under random bonds from the second-order regime of the pure 2d BC model, has the same values of critical exponents as the 2d Ising universality class, with the effect of the bond disorder on the specific heat being well described by double-logarithmic corrections, our findings thus supporting the marginal irrelevance of quenched bond randomness. Furthermore, the second-order transition, emerging under bond randomness from the first-order regime of the pure 2d BC model, was shown to belong to a distinctive universality class with $\nu = 1.30(6)$ and $\beta/\nu = 0.128(5)$. These results pointed to the existence of a strong violation of universality principle of critical phenomena, since these two second-order transitions, with different sets of critical exponents, are between the same ferromagnetic and paramagnetic phases.

In the current MC study, yielding also very accurate information, we wish to continue our investigations on the 3d BC model. We consider again a bimodal form of quenched bond randomness and we find different critical behaviors of the second-order phase transitions, emerging from the first- and second-order regimes of the pure model. Hence, in the present paper we offer additional evidence for the anticipated strong violation of universality. We will also constructively compare our findings to the existing literature on the effects of randomness in 3d systems, for which the pure versions undergo first- and second-order phase transitions. In the present MC study,

we employ a different numerical scheme based on cluster algorithms and parallel tempering (PT) and, as we will discuss in detail, this practice is a very good alternative for second-order phase transitions in disordered systems.

The relevant literature concerns mainly the 3d Ising model with quenched randomness, a clear case of the Harris criterion. The general random model has been extensively studied using MC simulations [13–25] but also field theoretical renormalization group approaches [26–28]. The diluted model has been treated in the low-dilution regime by analytical perturbative renormalization group methods [29–31] and a new fixed point, independent of the dilution, has been found. However, the first numerical studies suggested a continuous variation of the critical exponents along the critical line, but it became clear, after the work of Ref. [15], that the concentration-dependent critical exponents found in MC simulations are the effective ones, characterizing the approach to the asymptotic regime. Nowadays, the extensive numerical investigations of Ballesteros *et al.* [17], Berche *et al.* [22], and Fytas and Theodorakis [24] for the site-, bond-diluted, and random-bond versions of the model, have cleared out the doubts by presenting concrete evidence that the critical behavior of the 3d Ising model with quenched uncorrelated disorder is controlled by a new random fixed point, independent of the disorder strength value and the way this is implemented in the system. Moreover, both site- and bond-diluted Ising systems have been also studied by Hasenbusch *et al.* [20] in a high-statistics MC simulation, confirming universality and providing very accurate estimates of the critical exponents.

However, although the evidence of the existence of a unique universality class in the 3d random Ising model (RIM) is very strong, a full characterization of the types of models and the types of disorder that lead a transition into this class is still a challenging question. Such an interesting case is the $\pm J$ Ising model at the ferromagnetic-paramagnetic transition line, for which Hasenbusch *et al.* [25] have shown that it belongs also to the RIM universality class. Another relevant 3d random model is the site-diluted $q = 3$ Potts model which, in its pure version, is known to have a weak first-order phase transition. This model was studied by Ballesteros *et al.* [32] and it was clearly verified that the emerging under randomness second-order transition gives a definitively different magnetic exponent η . An analogous study on the 3d site-diluted $q = 4$ Potts model which, in its pure version, is known to exhibit a strong first-order phase transition has also produced results consistent with a further distinctive universality class [33]. The present study of the 3d random-bond BC model gives us the opportunity of a direct comparison with the above relevant 3d cases, by considering the emerging second-order transitions stemming from both its Ising-like continuous and its strong first-order transitions, making thus our attempt more appealing for understanding better the effect of disorder in 3d systems. Finally, it is to be noted that, although there

is a number of recent papers [34–37] dealing with the effects of randomness on the 3d ferromagnetic BC model, the present study appears to be the first attempting to clearly distinguish between the universality aspects of the ex-second- and ex-first-order regimes of the 3d random BC model.

The rest of the paper is laid out as follows: In the following Section we define the model (subsection II A) and we give a detailed description of our numerical approach (subsection II B) utilized to derive numerical data for large ensembles of realizations of the disorder distribution and lattices with linear sizes within the range $L \in \{8 - 44\}$. In subsection II B the finite-size scaling (FSS) scheme is described. In Sec. III we discuss the effects of disorder on the second-order phase transition regime of the model. Respectively, in Sec. IV we illustrate the conversion, under random bonds, of the originally first-order transition of the model to second-order and we present full details of our FSS attempts, that strongly point to a new distinctive universality class. Our conclusions are summarized in Sec. IV.

II. MODEL, SIMULATION, AND FINITE-SIZE SCALING SCHEMES

A. The random-bond Blume-Capel model

The pure BC model [38, 39] is defined by the Hamiltonian

$$H_p = -J \sum_{\langle ij \rangle} s_i s_j + \Delta \sum_i s_i^2, \quad (1)$$

where the spin variables s_i take on the values $-1, 0$, or $+1$, $\langle ij \rangle$ indicates summation over all nearest-neighbor pairs of sites, and $J > 0$ the ferromagnetic exchange interaction. The parameter Δ is known as the crystal-field coupling and to fix the temperature scale we set $J = 1$ and $k_B = 1$.

This model is of great importance for the theory of phase transitions and critical phenomena and besides the original mean-field theory [38, 39], has been analyzed by a variety of approximations and numerical approaches, in both $d = 2$ and $d = 3$. These include the real space renormalization group, MC renormalization-group calculations [40], ϵ -expansion renormalization groups [41], high- and low-temperature series calculations [42], a phenomenological FSS analysis using a strip geometry [43, 44], and of course MC simulations [11, 45–51]. As mentioned already in the introduction the phase diagram of the model consists of a segment of continuous Ising-like transitions at high temperatures and low values of the crystal field which ends at a tricritical point, where it is joined with a second segment of first-order transitions between (Δ_t, T_t) and $(\Delta_0, T = 0)$. For the simple cubic lattice, considered in this paper, $\Delta_0 = 3$. The location of the tricritical point has been estimated by Deserno [48] using microcanonical MC approach as

the point $[\Delta_t, T_t] = [2.84479(30), 1.4182(55)]$, and to a better accuracy by the more recent estimation of Deng and Blöte [50] as $[\Delta_t, T_t] = [2.8478(9), 1.4019(2)]$.

In the random-bond version of the BC model, studied in this paper, the bond disorder follows the bimodal distribution

$$P(J_{ij}) = \frac{1}{2} [\delta(J_{ij} - J_1) + \delta(J_{ij} - J_2)] ; \quad (2)$$

$$\frac{J_1 + J_2}{2} = 1 ; \quad J_1 > J_2 > 0 ; \quad r = \frac{J_2}{J_1} ,$$

where the parameter r reflects the strength of the bond randomness (ratio of interaction strengths in a fixed 50%/50% weak/strong bonds mixing). The resulting quenched disordered version of the model reads now as

$$H = - \sum_{\langle ij \rangle} J_{ij} s_i s_j + \Delta \sum_i s_i^2. \quad (3)$$

Since we aim at investigating the effects of bond randomness on the segments of continuous Ising like and first-order transitions of the original pure model, we have to choose suitable values of the crystal field Δ and the disorder parameter r . For the first-order regime, we are looking for a convenient strong disorder combination, strong enough to convert the originally first-order transition to a second-order one. The value $\Delta = 2.9$ is a convenient choice, since it is well inside the region of first-order transitions (see the above mentioned location for the tricritical point). At this value of Δ we have numerically verified that the disorder strength $r = 0.5/1.5 = 1/3$ is strong enough to convert, without doubt, the original first-order transition to a genuine second-order transition. Thus, we will consider, in the sequel, the cases $(\Delta, r) = (1, 1/3)$ and $(\Delta, r) = (2.9, 1/3)$, which correspond to the ex-second- and ex-first-order regimes. These cases serve very well our purposes to study the universality aspects of the emerging under bond-randomness second-order phase transitions of the model.

B. Reviews of Monte Carlo and finite-size scaling schemes

The accuracy of MC data may be decisive for a successful FSS estimation of critical properties and the proper selection of an algorithm is the basic requirement for the generation of accurate MC data. Thus, over the years, the numerical estimation of critical exponents has been a non-trivial exercise, even for the simplest models, such as the Ising model. An appropriate algorithm close to a critical point has to overcome the well-known effects of critical slowing down, and some otherwise excellent and exact algorithms, such as the Metropolis algorithm [52], which work adequately far from the critical point, become inefficient close to it. It is also well known that, an approach via importance sampling, close to a second-order phase transition, requires appropriate use of cluster

algorithms that can efficiently overcome the critical slowing down effects. Wolff-type algorithms [53–55] belong to this category, are easy to implement, and also very efficient close to critical points.

Since, in the present paper, we wish to simulate the random-bond BC model close to critical points, the implementation of the Wolff algorithm could be a suitable alternative. However, for the BC model the Wolff algorithm can not be used alone, because Wolff steps act only on the non-zero spin values. A suggested practice is now a hybrid algorithm along the lines followed by Ref. [49]. An elementary MC step (MCS) of this hybrid scheme consists of a number of Wolff steps (typically 5 Wolff-steps) followed by a Metropolis sweep of the lattice, whereas the usual MCS for the Metropolis algorithm is just one lattice sweep. The combination with the Metropolis lattice sweep is dictated by the fact that the Wolff steps act only on the non-zero spin values. The proposed hybrid algorithm is, of course, one of several alternatives for the study of the BC model. We note in passing that, in our previous analogous studies of the square lattice pure and random-bond BC model [11] we have been using a sophisticated two-stage Wang-Landau approach, very efficient for studying at the same time characteristics of the first- and second-order regimes of the model.

However, since the present study concerns only the behavior close to the emerging, under bond randomness, critical points, the described hybrid approach, combined with a PT protocol, which will be detailed below, is much more appealing and its convergence may be easily checked. Thus, we have simulated the random-bond BC model on the simple cubic lattice for the cases $(\Delta, r) = (1, 1/3)$ and $(\Delta, r) = (2.9, 1/3)$ and for lattice sizes in the range $L = 8 - 44$, by implementing the hybrid approach described above, suitably adapted to the present disordered model. As is always the case, the simulation task for a disordered system, such as the present random-bond BC model, is by far more demanding than its pure counterpart, since one has to sum over disorder realizations. Furthermore, for the random-bond model the simple Wolff algorithm cannot be applied and a suitable generalization is necessary. This generalization is a straightforward adaption of the Wolff algorithm by introducing two different probabilities for putting links between sites; corresponding to the weak and strong nearest-neighbor ferromagnetic interactions. It is then rather easy to show that, the generalized cluster algorithm has all the properties of the original Wolff algorithm.

In order to extract information on the critical properties of the random-bond BC model, we are going to apply the ideas of FSS. For the estimation of the critical temperatures and the corresponding critical exponents, one has to generate MC data to cover several finite-size anomalies of the finite systems of linear size L . The above described hybrid approach has to be carried over to a certain temperature range depending on the lattice size. These temperatures may be selected independently or it

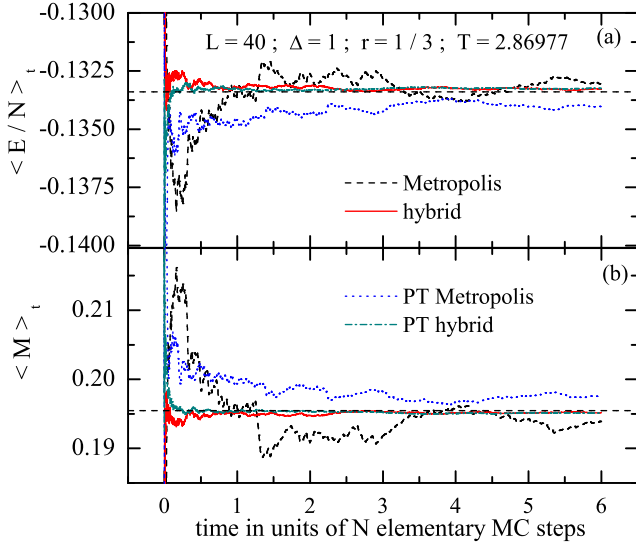


FIG. 1: (color online) Behavior of moving averages for the energy per site $\langle E/N \rangle_t$, in panel (a), and the order parameter $\langle M \rangle_t$, in panel (b), at a selected temperature, close to the critical. The behavior of the four simulation schemes is illustrated and the definition of elementary steps is discussed in the text.

may also be convenient, and accurate, to implement a PT protocol. Such a PT protocol, based (mainly) on temperature sequences corresponding to an exchange rate 0.5, was tested for both cases considered in this work, i.e. $(\Delta, r) = (1, 1/3)$ and $(\Delta, r) = (2.9, 1/3)$, and was found to be very accurate. We should point out here that, the proposed PT approach is very close to the practice suggested recently in Ref. [56]. Furthermore, a similar approach has been followed recently for a very successful estimation of critical properties of the Ising and the $S = 1$ model (BC) on some Archimedean lattices [57]. Appropriate temperature sequences, for the application of a hybrid PT protocol were generated via short preliminary runs. During these preliminary runs a simple histogram method [53, 54] was applied to yield energy probability density functions and from these, the appropriate sequences of temperatures were easily determined, following the recipe of Ref. [56]. The preliminary runs were applied to only one disorder realization, but it was checked that the resulting temperature sequences were producing, to an excellent approximation, a constant exchange rate of 0.5 for the PT protocol, when applied to any other different disorder realization. This is of course an intrinsic, and very convenient property of the present random-bond model.

The above MC scheme was carefully tested almost for all lattice sizes before its implementation for the generation of MC data necessary for applying FSS. These

tests included two basic ingredients: the first was the estimation of the MC times necessary for equilibration and thermal averaging process applied to a particular disorder realization and the second involved the observation of running sample-averages of some thermodynamic quantity, such as for instance, the magnetic susceptibility, at some particular temperature close to the critical one. These tests, not only provided convincing evidence for a successful determination of equilibrium results, but also highlighted the way towards an efficient and optimum scheme. For instance it was checked that for a rather small lattice size, such as $L = 16$, the sample averages over 150 disorder realizations of all thermodynamic quantities were identical, irrespective of the algorithm used (simple Metropolis or hybrid algorithm), provided one uses reasonable MC times for equilibration and thermal averaging. This could be explained as a result of effective cancellation of statistical errors from the sample-averaging process. Noteworthy, that sample-to-sample fluctuations are much larger than any usual statistical errors in a proper MC thermal averaging process. Of course, for a particular disorder realization the difference in the outcome of different algorithms may be truly spectacular.

In fact, we can observe the superiority of the hybrid approach, over a simple Metropolis scheme [52], in Fig. 1. This figure is constructed by using moving averages for the energy per site ($\langle E/N \rangle_t$) and the order parameter ($\langle M \rangle_t$) for a lattice size $L = 40$ at a selected temperature, close to the critical temperature, for the case $(\Delta, r) = (1, 1/3)$ of the random-bond BC model. As it can be seen from this illustration, the Metropolis algorithm suffers from very strong fluctuations and so does the corresponding PT protocol (applied in a temperature sequence including the temperature shown) using this algorithm. They both follow a very slow approach to equilibrium and only with the help of extensive sampling one could expect results of reasonable accuracy. On the other hand, the hybrid approach converges very fast to equilibrium and produces quite accurate results. The corresponding PT hybrid algorithm appears to further improve this good behavior, which is a reasonable expectation, since the PT approach should be in general more effective for disordered systems. Note also that, Fig. 1 is constructed by using one particular disorder realization and the dashed straight lines in the panel of the figure indicate the final average values of four independent PT hybrid runs of the same realization, whereas the fluctuating lines correspond to one single run for each algorithm. A careful examination of this illustration shows that even a single run for the thermal averaging process is very accurate for the hybrid and the PT hybrid algorithms and for the presented case, a MC time of the order of $3 \times N$, is adequate and optimum for the thermal process. The corresponding equilibration MC times are always shorter than this. There is no doubt that, the use of the hybrid algorithm is essential for the study of the present model.

Let us review now details from the FSS tools used

throughout the paper, for the estimation of critical properties of the disordered system. The outline below follows our previous studies on random-bond models and is very close to the traditional standard tools of the theory of FSS. When studying a disordered system, a large number of disorder realizations has to be used in the summations in order to obtain good sample-averages of any basic thermodynamic quantity Z , which is a usual thermal average of a single disorder realization. The sample (or disorder) averages may be then denoted as $[Z]_{av}$ and their finite-size anomalies respectively as $[Z]_{av}^*$. These (disorder-averaged) finite-size anomalies will be used in our FSS attempts, following a quite common practice [33] and their temperature locations will be denoted by $T_{[Z]_{av}^*}$. Thus, we also follow the conventional numerical approach that appears to work well for the present model, at both the ex-second- and ex-first-order regimes, at the disorder strength values considered. However, in an alternative approach [18] one may consider individual sample dependent maxima (anomalies) and the corresponding sample dependent pseudocritical temperatures. This alternative route is far more demanding computationally, but the corresponding FSS analysis may be more precise, and additional useful information concerning the properties of disorder averages becomes available. Our study addresses only exponents describing the disorder-averaged behavior and we do not use a FSS analysis based on sample dependent pseudocritical temperatures. For disordered systems one can make a clear distinction between typical and averaged exponents [58, 59]. An extreme example of this case with very pronounced differences in the corresponding ν exponents has been provided, and critically discussed, by Fisher [58] on the random transverse-field Ising chain model. Finally, disordered critical phenomena are known to display in general multicritical exponents [60, 61] and we shall return to this interesting point in our last section, when discussing the violation of universality in the present model.

The number of disorder realizations and the selection of temperatures may influence the accuracy and suitability of the MC data from which the locations of the finite-size anomalies are determined, by fitting a suitable curve (for instance a fourth-order polynomial) in the neighborhood of the corresponding peak. Since we are implementing a PT hybrid approach, based on temperatures corresponding to an exchange rate 0.5, we are selecting certain temperature sequences consisting of a number of (say 3 or 5) different temperatures, averaging then over a relatively moderate number (~ 100) of disorder realizations. This yields a number of (3 or 5) points of the averaged curves $[Z]_{av}$. This set of points may not be adequately dense and will not cover the ranges of the peaks of all thermodynamic quantities of interest. Therefore, this procedure is repeated several times (depending on the linear size L) by using new sets of temperatures which are translated with respect to the previous sets. These translations should be carefully chosen so that a final dense set of points, suitable for all finite-size anomalies,

is obtained. This corresponds, on average, to a very large number of realizations, since for each PT hybrid run, a different set of disorder realizations was used. We have found this practice very convenient, efficient, and most importantly quite accurate. Thus, we were able to describe the averaged finite-size anomalies of the system with high accuracy.

In order to estimate the critical temperature, we follow the practice of simultaneous fitting approach of several pseudocritical temperatures [11]. From the MC data, several pseudocritical temperatures are estimated, corresponding to finite-size anomalies, and then a simultaneous fitting is attempted to the expected power-law shift behavior $T_{[Z]_{av}^*} = T_c + b_Z \cdot L^{-1/\nu}$. The traditionally used specific heat and magnetic susceptibility peaks, as well as the peaks corresponding to the following logarithmic derivatives of the powers $n = 1, 2$, and $n = 4$ of the order parameter with respect to the inverse temperature $K = 1/T$ [62],

$$\frac{\partial \ln \langle M^n \rangle}{\partial K} = \frac{\langle M^n H \rangle}{\langle M^n \rangle} - \langle H \rangle, \quad (4)$$

and the peak corresponding to the absolute order-parameter derivative

$$\frac{\partial \langle |M| \rangle}{\partial K} = \langle |M| H \rangle - \langle |M| \rangle \langle H \rangle, \quad (5)$$

will be implemented for a simultaneous fitting attempt of the corresponding pseudocritical temperatures. Furthermore, the behavior of the crossing temperatures of the fourth-order Binder's cumulant [63], and their asymptotic trend, will be observed and utilized for a safe estimation of the critical temperatures.

The above described simultaneous fitting approach provides also an estimate of the correlation length exponent ν . An alternative estimation of this exponent is obtained from the behavior of the maxima of the logarithmic derivatives of the powers $n = 1, 2$, and $n = 4$ of the order parameter with respect to the inverse temperature, since these scale as $\sim L^{1/\nu}$ with the system size [62]. Once the exponent ν is well estimated, the behavior of the values of the peaks corresponding to the absolute order-parameter derivative, which scale as $\sim L^{(1-\beta)/\nu}$ with the system size [62], gives one route for the estimation of the magnetic exponent ratio β/ν . Additionally, knowing the exact critical temperature, or very good estimates of it, we can utilize the behavior of the order parameter at the critical temperature for the traditionally effective estimation of the exponent ratio β/ν ($M_c = M(T = T_c) \sim L^{-\beta/\nu}$). Summarizing, our FSS approach utilizes, besides the traditionally used specific heat and magnetic susceptibility maxima, the above four additional finite-size anomalies for an accurate estimation of critical temperatures and relevant exponents.

III. EX-SECOND-ORDER REGIME: UNIVERSALITY CLASS OF THE RANDOM ISING MODEL

We study in this Section the 3d random-bond BC model at the second-order regime of the phase diagram. We have considered the case $(\Delta, r) = (1, 1/3)$ and simulated lattices with linear sizes in the range $L = 8 - 44$. Below we discuss in detail our efforts to find a comprehensive FSS scheme to fit the numerical data. However, before illustrating details of our study, it is useful to recall again that, according to general universality arguments, the pure BC model at $\Delta = 1$ is expected to belong to the 3d Ising universality class and thus, the case studied here, should be contrasted to the relevant literature on the 3d RIM. From the relevant literature, it appears that a consensus have been achieved today with regard to the existence of a single universality class for the general 3d RIM [17, 22, 24, 25]. However, it is also true that the study of Berche *et al.* [22] on the 3d bond-diluted Ising model, has emphasized the strong influence of crossover phenomena and pointed out that the identification of this universality class is a very difficult task. For the case of magnetic bond concentration $p = 0.7$, studied in that paper, these authors found an effective exponent $(1/\nu)_{eff} = 1.52(2)$. Correspondingly, for the case $p = 0.55$ the effective value was found to be $(1/\nu)_{eff} = 1.46(2)$. This noticeable variation in the effective exponents indicated possible confluent corrections and/or crossover terms [22]. They finally agreed that, the case $p = 0.55$ appears to be the case of least scaling corrections and thus, in this way, agreement with the value given by Ballesteros *et al.* [17] was established.

The problem of slowing decaying scaling corrections has been discussed in detail for both these randomly site- and bond-diluted systems by Hasenbusch *et al.* [20], and for the latter, the value $p = 0.54(2)$ has been proposed as the value at which the leading scaling corrections vanish. The above observations will be very useful later in this Section, when we discuss our problems in extracting a reliable estimate of this exponent, since we have faced similar problems. Noteworthy that, in a systematic study of the $\pm J$ Ising model at the ferromagnetic-paramagnetic transition line, Hasenbusch *et al.* [25] have analyzed the effects of leading and next-to-leading scaling corrections and proposed a value of the concentration of the ferromagnetic lines of this model at which corrections to scaling almost vanish. The final estimate for the correlation length exponent determined by this study is almost identical with the value given by Ballesteros *et al.* [17].

We start the FSS analysis by attempting the estimation of the exponent ratio that characterizes the divergence of the susceptibility. We assume that the (sample-averaged) susceptibility obeys a simple power law of the form $[\chi_T]_{av}^* = b \cdot L^{\gamma/\nu}$. The fitting attempts are found to be quite stable with respect to the size range chosen. We attempted the ranges $L = 8 - 44$, $12 - 44$, \dots , $28 - 44$

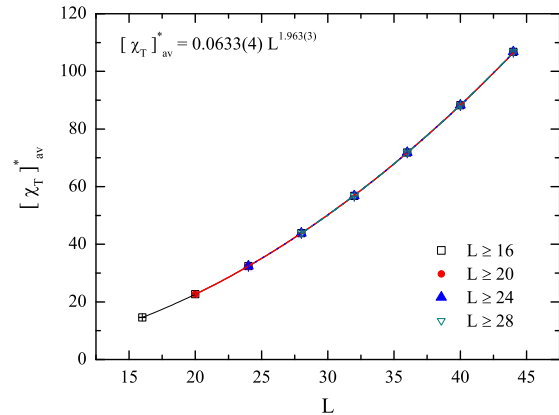


FIG. 2: (color online) Illustration of the divergence of the susceptibility maxima by a simultaneous global fitting attempt on the data corresponding to several lattice-size ranges shown in the panel, indicated by the different line colors.

and observed the behavior of the resulting coefficients b and exponents γ/ν . The estimates of the exponent vary slowly in the range $\gamma/\nu = 1.962 - 1.967$, as we increase L_{min} from $L_{min} = 8$ to $L_{min} = 28$. A kind of mean value estimate can be obtained by a global fitting attempt simultaneously applied to the above ranges. Such a simultaneous attempt using the ranges $L = 16 - 44$, $20 - 44$, $24 - 44$, and $L = 28 - 44$ is shown in Fig. 2 giving an estimate $\gamma/\nu = 1.963(3)$. The illustrated estimate is in full agreement with the values given by Ballesteros *et al.* [17] and Berche *et al.* [22]. Finally, observing the over all trend of such simultaneous fitting attempts we shall propose as our final estimate $\gamma/\nu = 1.964(4)$, in coincidence with the estimate $\gamma/\nu = 1.965(10)$ given by Berche *et al.* [22] for the case $p = 0.7$ mentioned above.

A similar simple power-law behavior was found for the peaks corresponding to the absolute order-parameter derivative which scale as $\sim L^{(1-\beta)/\nu}$. Since the examined behavior, in this case, is very similar to the above behavior, we shall not discuss further our efforts and give only our final estimate for the relevant exponent $(1 - \beta)/\nu = 1.022(5)$. Combining the above estimates and assuming at this point hyperscaling - in the form: $2/\nu = 2(1 - \beta)/\nu + (d - \gamma/\nu)$ - we find $1/\nu = 1.54(1)$. In the following we will see that, this value is not far from the effective estimates determined below from the shift behavior of the system.

Let us now attempt the estimation of the correlation length exponent via the scaling behavior of the logarithmic derivatives of the powers $n = 1, 2$, and $n = 4$ of the order parameter with respect to the inverse temperature [see Eq. (4)]. Their behavior was observed to be quite successfully fitted to a stable simple power law with rather small variation of the effective critical exponent. All the estimates were close to the above value $1/\nu = 1.54$ and for illustrative reasons we have presented one such

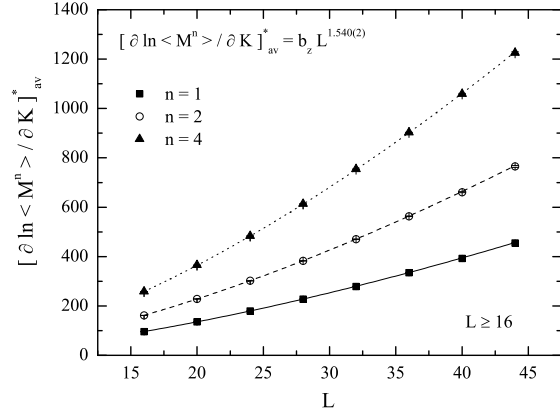


FIG. 3: FSS behavior of the peaks of the logarithmic derivatives of the powers $n = 1, 2$, and $n = 4$ of the order parameter with respect to the inverse temperature. The estimate for the exponent $1/\nu$ is given in the panel by applying a simultaneous fitting attempt to a simple power law in the size range $L = 16 - 44$.

simultaneous fitting attempt in Fig. 3. Therefore, the scheme appears to be in good agreement with hyperscaling. We turn now to the estimation of this exponent from the general shift behavior of the system.

As is well known, the pseudocritical temperatures, corresponding to several finite-size anomalies, provide a traditional route for the estimation of the critical temperature and the correlation length exponent. A simultaneous fitting attempt to a power-law shift behavior of the form $T_{[Z]_{av}}^* = T_c + b_Z \cdot L^{-1/\nu}$ is often the attempted practice. For the present case the following temperatures were calculated. Temperatures of the peaks of the specific heat, magnetic susceptibility, inverse temperature derivative of the absolute order parameter, and inverse temperature logarithmic derivatives of the $n = 1, 2$, and $n = 4$ powers of the order parameter. The data were fitted in the ranges $L = 8 - 44$ to $L = 28 - 44$ and the behavior of the estimates was observed. With the exception of the fitting attempt corresponding to $L = 8 - 44$, which gave an estimate $1/\nu = 1.465(1)$, all other attempts gave fluctuating estimates in the range $1/\nu = 1.52 - 1.54$, which seems to agree well with the previous finding. Yet, at the same time, we observed a noticeable shift of the estimated critical temperature from values $T_c = 2.8798$ to $T_c = 2.88015$ as we varied L_{min} from $L_{min} = 8$ to $L_{min} = 28$. Here, a careful examination of the behavior of the fourth-order Binder's cumulant of the order parameter $[V_T]_{av} = [1 - \langle M^4 \rangle / 3 \langle M^2 \rangle^2]_{av}$ suggested that a larger critical temperature in the range $T_c = 2.88015 - 2.88045$ may be a very strong option. Figure 4 is a very clear illustration of this statement, since it demonstrates that, at the temperature $T_c = 2.88035$, the behavior of the cumulant is almost independent of L .

In order to better understand the shift-behavior of

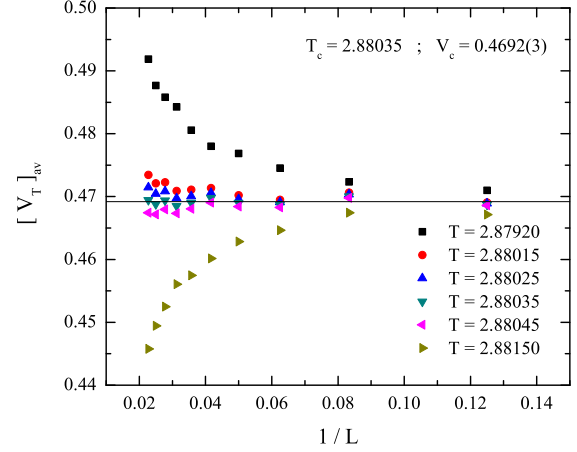


FIG. 4: (color online) Illustration of the asymptotic trend of the fourth-order Binder's cumulant of the order parameter for various temperatures close to the critical temperature. Note the stability of the estimates at $T_c = 2.88035$.

the system and present a global illustration of it, we fix the critical temperature to several values and calculate effective exponents. We studied their size dependence by varying L_{min} as usual, from $L_{min} = 12$ to $L_{min} = 28$, and by further applying simultaneous fitting attempts using the form $T_{[Z]_{av}}^* = T_c + b_Z \cdot L^{-1/\nu}$ with fixed critical temperatures from the set $T_c = \{2.88015, 2.88025, 2.88035, 2.88045, 2.8807\}$. The resulting global behavior is now illustrated in Fig. 5. This figure clearly indicates that effective exponents are very sensitive to small temperature changes. Furthermore, by applying a linear fitting in the effective estimates for $L \geq 16$ for the case $T_c = 2.88035$ we obtain $1/\nu = 1.504$ and this is indicated by the bold straight line in the panel, as our central estimate for the exponent. Repeating the same procedure for the case $T_c = 2.88025$ we obtain $1/\nu = 1.539$, whereas for the case $T_c = 2.88045$ we obtain the value $1/\nu = 1.466$. We may use these remote estimates as upper and lower bounds respectively of our exponent estimation and these are indicated in the panel by the dotted lines. For the sake of comparison we show also in the panel the accepted limits for the estimation of the critical exponent $1/\nu$ of the pure 3d Ising model $\nu = 0.6304(13)$ [64] and the 3d RIM $\nu = 0.6837(53)$ [17]. Based on the above observations, one could anticipate that any estimate in the range $1/\nu = 1.466 - 1.539$, indicated by the dotted lines in the panel, should be acceptable. We point out here that, the exponent for the pure 3d Ising model, $\nu = 0.6304(13)$ [64] illustrated in Fig. 5, is a moderate estimate with rather large error bounds. A most recent and accurate estimate is $\nu = 0.63002(10)$, obtained by Hasenbusch [65] in excellent agreement with other recent studies of the 3d Ising model [66, 67].

Overall, the present case shares many of the problems

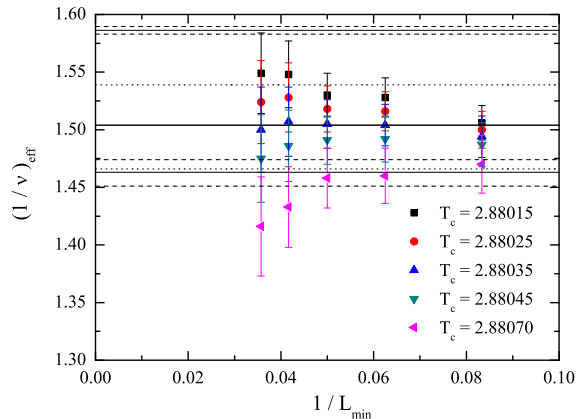


FIG. 5: (color online) A global illustration of the estimates of the effective exponent $(1/\nu)_{eff}$. The solid line drawn in the panel close to the value $1/\nu = 1.586$, together with the dashed lines, illustrate the location of the critical exponent range for the pure 3d Ising model. The analogous range for the 3d RIM is drawn close to the value $1/\nu = 1.463$. The range $1/\nu = 1.466 - 1.539$ (dotted lines in the panel) around the heavy solid line at the value $1/\nu = 1.504$ demonstrate the possible asymptotic evolution of the critical exponent for the present model.

encountered by Berche *et al.* [22] in their study of the 3d bond-diluted Ising model for the case of magnetic bond concentration $p = 0.7$. However, the above illustrations show that, despite the already mentioned problems, our data are compatible with the general expectations of the general 3d RIM. We close this Section with two additional comments. Firstly, we also tried to observe the shift behavior by fixing the shift exponent to the value $1/\nu = 1.463$ proposed by Ballesteros *et al.* [17]. We then found that the corresponding simultaneous fitting attempts gave values for the critical temperatures which are slowly approaching the value $T_c = 2.88035(10)$ suggesting once again that this may be the asymptotic critical temperature. Secondly, we observed the FSS behavior of the order parameter by fixing the critical temperature to the values from the set $T_c = \{2.88015, 2.88025, 2.88035, 2.88045\}$. The estimated effective exponents β/ν , had in all cases values in the ranges $\beta/\nu = 0.51(1) - 0.52(1)$. These values, together with the earlier estimate $\gamma/\nu = 1.964(4)$, satisfy quite well hyperscaling.

IV. EX-FIRST-ORDER REGIME: DISORDER-INDUCED SECOND-ORDER PHASE TRANSITION

In this Section we investigate the effects of bond randomness on the segment of the first-order transitions of the original pure model. At the value $\Delta = 2.9$, which

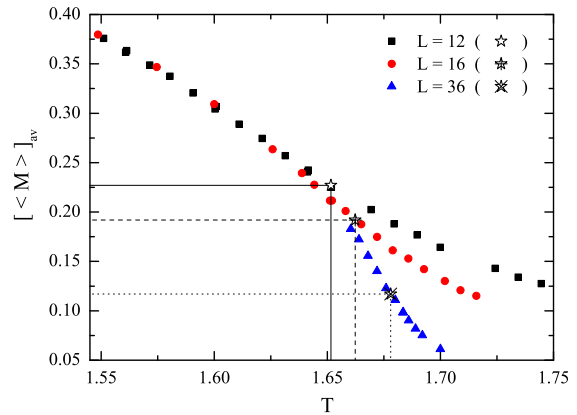


FIG. 6: (color online) Illustration of the continuous behavior of the order parameter for the random-bond BC model at $(\Delta, r) = (2.9, 1/3)$. Three different lattice sizes $L = 12$, 16 , and $L = 36$ are shown and the illustrated behavior is approximately centered at the temperatures corresponding to the peaks of the magnetic susceptibility, indicated by the asterisks and the drop lines.

is well inside the first-order regime of the pure model, we have numerically verified that the disorder strength $r = 1/3$ is strong enough to convert, without doubt, the original first-order transition to a genuine second-order one. The illustration in Fig. 6 consists very clear evidence of this statement. In this figure we show the behavior of the order parameter close to the pseudocritical region for three different lattice sizes $L = 12$, 16 , and $L = 36$. The three different asterisks and the respective drop lines indicate the points on these curves corresponding to the magnetic susceptibility peaks. These order-parameter curves, at the corresponding pseudocritical regions, are smooth and no sign of discontinuity appears as the lattice size increases to $L = 36$. Since the order parameter is continuous at the combination $(\Delta, r) = (2.9, 1/3)$, the disorder-induced transition is a second-order phase transition, which we will take as representative of the ex-first-order universality class.

For the case $(\Delta, r) = (2.9, 1/3)$, we start the FSS analysis by attempting the estimation of the exponent ratio that characterizes the divergence of the susceptibility. First, we assume that the (sample-averaged) susceptibility obeys a simple power law of the form $[\chi_T]_{av}^* = b \cdot L^{\gamma/\nu}$. However, the fitting attempts are found to be unstable with respect to the size range (we attempted the ranges $L = 8 - 44$, $12 - 44$, ...) and the resulting coefficients b and exponents γ/ν are varying in a competitive way, indicating the need of correction terms. Therefore, we tried to find a resolution of this problem by introducing correction terms and we found that a constant background term, was actually the most effective in eliminating the observed instability. The behavior of the corresponding fitting attempts, assuming the scaling relation

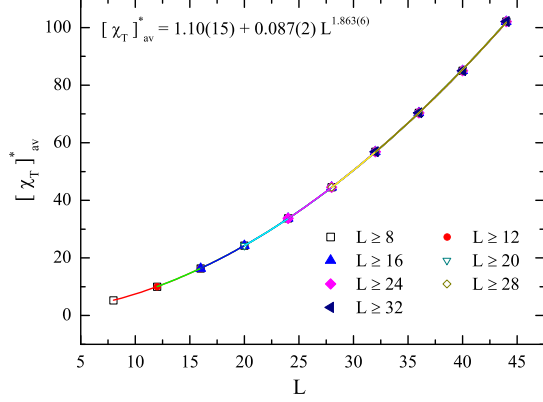


FIG. 7: (color online) The divergence of the susceptibility maxima is well described by a scaling law of the form $[\chi_T]_{av}^* = a + b \cdot L^{\gamma/\nu}$. Illustration of a simultaneous global fitting attempt on the data corresponding to several size ranges shown in the panel, indicated by the different line colors. Note that, the simultaneous attempt gives an estimate of $a = 1.10(15)$ which is in agreement, within errors, with all separate attempts and effectively coincides with the estimates of the ranges $L = 8 - 44$ and $L = 12 - 44$.

$[\chi_T]_{av}^* = a + b \cdot L^{\gamma/\nu}$, is very good and produces very slowly varying fitting parameters. A completely stable behavior was obtained by fixing the value of the background term to be of the order of $a = 1.0 - 1.2$. The values of the background term for the first two ranges $L = 8 - 44$ and $L = 12 - 44$, and the value obtained by a simultaneous global fitting attempt on the data corresponding to several size ranges, as shown in Fig. 7, are effectively the same. As indicated in the panel of this figure the global attempt gives an estimate $a = 1.10(15)$. In the same panel we give the estimates of $b = 0.087(2)$ and the exponent $\gamma/\nu = 1.863(6)$. Using this value ($a = 1.1$) we illustrate in Fig. 8 the stability of the resulting scaling scheme by presenting, in a double logarithmic scale, the behavior of the two most remote ranges $L = 8 - 44$ and $L = 28 - 44$. The coincidence of the estimates in this panel appears as a guaranty of the quite accurate estimation of the magnetic exponent ratio $\gamma/\nu = 1.864(12)$.

However, it may be crucial for future studies to give here a more detailed discussion on the various corrections tested before adopting the above scenario. Our fitting attempts followed a quite common practice restricting the search to an expression including only one correction term, e.g., $[\chi_T]_{av}^* = b \cdot L^{\gamma/\nu} + b' \cdot L^{\gamma/\nu - \epsilon}$. This restriction was unavoidable, since the fits were already notoriously unstable, as we increased the minimum lattice size, with the above four-parameter expression. The stability and quality of the fittings were then observed by fixing the correction exponent ϵ to various relevant values and treating only the exponent γ/ν as a free one. The quality of the fittings was characterized by their cu-

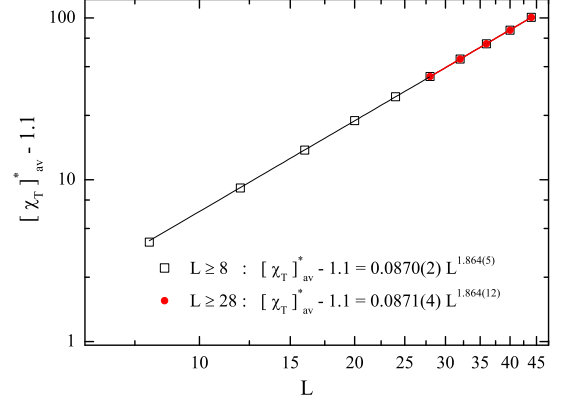


FIG. 8: (color online) This figure is complementary to Fig. 7 and further illustrates the stability of the scaling scheme by presenting, in a log-log scale, the behavior of the two most remote ranges $L = 8 - 44$ and $L = 28 - 44$. Note that, we have here subtracted from the susceptibility data the estimated value of the background term ($a = 1.1$).

mulated square deviation, χ^2 , and the stability of the values of the exponent γ/ν and the corresponding amplitudes were observed. The best sequence of fittings was obtained for $\epsilon = \gamma/\nu$, corresponding to the regular background behavior adopted in this paper and illustrated in Figs. 7 and 8. This choice is unique, in the sense that is for sure the simplest one. Besides, all the other tested values of ϵ , in the neighborhood of the leading and next-to-leading corrections to scaling, corresponding to the 3d RIM $\epsilon = \omega = 0.33(3)$, $\epsilon = 2\omega = 0.66(6)$ and $\epsilon = \omega_2 = 0.82(8)$ [20], did not produce a stable sequence of fittings, but gave a rather pathological variation of the estimates of the exponent γ/ν and the relevant amplitudes. Yet, one may also observe the stability and quality of the fittings by fixing both the exponent γ/ν and the exponent ϵ . In these final attempts, we did find cases of comparable quality and stability that are completely compatible with the 3d RIM universality class. One such case is described by the expression $[\chi_T]_{av}^* = 0.0494(4) \cdot L^{1.964} + 0.013(1) \cdot L^{1.964-0.66}$, and another one is described by the expression $[\chi_T]_{av}^* = 0.052(2) \cdot L^{1.964} + 0.18(2) \cdot L^{1.964-0.82}$. The above two expressions and the behavior in Fig. 8 produce very close values (almost identical within statistical errors) in the range $L = 8 - 44$ studied in this paper. This observation should serve also as a warning of the difficulties and the pathology of the fitting attempts, since the existence of stable forms, with quite different correction exponents, means also that a completely reliable estimation of corrections-to-scaling exponents may not be feasible even at larger lattice sizes.

Let us now investigate the FSS behavior of the peaks corresponding to the absolute order-parameter derivative which, as mentioned earlier, are expected to scale

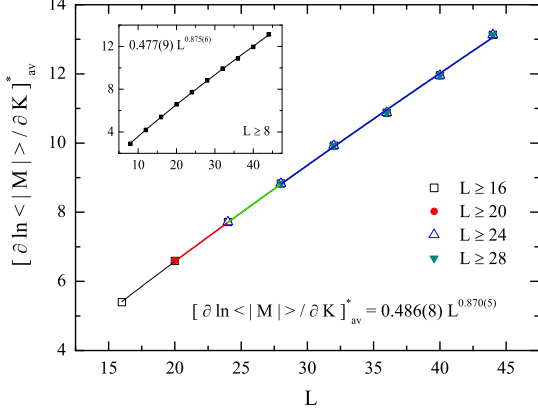


FIG. 9: (color online) Illustration of a simultaneous global fitting attempt on the data corresponding to several size ranges shown in the panel for the maxima of the sample-averaged absolute order-parameter derivative. Note that in this case, the fitting attempts are insensitive to the size ranges used.

as $\sim L^{(1-\beta)/\nu}$ with the lattice size. Here, we find that, the corresponding maxima obey very well a simple power law $[\partial \langle |M| \rangle / \partial K]_{av}^* = b \cdot L^{(1-\beta)/\nu}$ without any correction terms. The corresponding fitting attempts are very stable with respect to the lattice-size range, as moving from $L = 8 - 44$ to $L = 28 - 44$. Figure 9 illustrates in the main panel a simultaneous global fitting attempt on the data corresponding to the size ranges shown. The inset of this figure presents a simple fitting for the complete lattice range $L = 8 - 44$. The estimates for the exponent are almost insensitive to the used lattice-size ranges giving for the simultaneous global fitting $(1 - \beta)/\nu = 0.870(5)$ and for the simple fitting $L = 8 - 44$, in the inset, $(1 - \beta)/\nu = 0.875(6)$. These results indicate the consistency of the FSS scheme and the accuracy of the numerical data. We may take as a final (quite confident and moderate in its error bounds) estimate, the value $(1 - \beta)/\nu = 0.87(1)$.

As mentioned earlier, the pseudocritical temperatures, corresponding to several finite-size anomalies, provide a route for the estimation of the critical temperature and the correlation length exponent. A simultaneous fitting attempt to a power-law shift behavior of the form $T_{[Z]_{av}}^* = T_c + b_Z \cdot L^{-1/\nu}$ is the generally suggested practice. Figure 10 illustrates the shift behavior of such several pseudocritical temperatures. These temperatures correspond to the peaks of the following six (sample-averaged) quantities: specific heat, magnetic susceptibility, inverse temperature derivative of the absolute order parameter, and inverse temperature logarithmic derivatives of the $n = 1$, $n = 2$, and $n = 4$ powers of the order parameter. The data illustrated are fitted in the range $L = 12 - 44$, which corresponds to the best fitting attempt of all tried. The resulting estimates of the critical temperatures and the shift exponent $1/\nu$ are given in the panel. However,

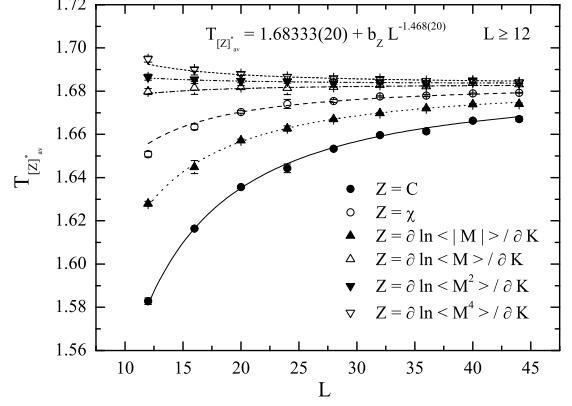


FIG. 10: FSS behavior of the pseudocritical temperatures defined in the text. Estimates for the critical temperatures and the shift exponent $1/\nu$ are given in the panel. The stability of the fitting scheme is discussed in the relevant text.

in this case also, the fitting attempts for the estimation of the critical exponent $1/\nu$ from the data of the pseudocritical temperatures are not completely stable. Therefore, some further comments and analysis are necessary. Despite that, the estimation of the critical temperature is quite stable, with values ranging from $T_c = 1.6833(2)$ to $T_c = 1.6835(2)$, as we vary the lattice-size ranges from $L = 8 - 44$ to $L = 24 - 44$. However, the corresponding exponent estimates $1/\nu$ have a noticeable variation with estimates from $1.51(2)$ to $1.42(2)$. The statistical errors influence here the quality but also the stability of the fitting attempts.

To better understand the shift-behavior we tried the following two assumptions. First, we fixed the critical temperature to be $T_c = 1.6835$, a value indicated also by a very careful examination of the behavior of the fourth-order Binder's cumulant of the order parameter (not shown here for brevity). Again, we found a similar variation as above with the lattice-size ranges used. The best fittings were obtained for the ranges $L = 12 - 44$ and $L = 16 - 44$, giving also very close estimates for the shift exponent $1/\nu$ [$1/\nu = 1.45(2)$]. Subsequently, we tried to observe the behavior of the estimates of the critical temperature by fixing the shift exponent to the value $1/\nu = 1.438$. This is the value obtained by satisfying hyperscaling, given the previous estimates for $\gamma/\nu = 1.864$ and $(1 - \beta)/\nu = 0.87$. The estimates for the critical temperature are all very close to $T_c = 1.68345$ and the best fitting attempt, giving also an estimate with the smallest error, is $T_c = 1.6835$, corresponding to the range $L = 12 - 44$. We have therefore accepted as our best estimation of the shift behavior the values $T_c = 1.6835(2)$ and $1/\nu = 1.45(2)$.

An independent estimation of the correlation length exponent can be obtained via the scaling behavior of the logarithmic derivatives of the powers $n = 1$, 2 , and $n = 4$

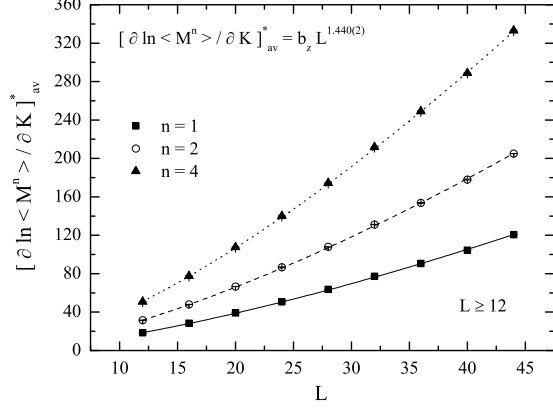


FIG. 11: FSS behavior of the peaks of the logarithmic derivatives of the powers $n = 1, 2$, and $n = 4$ of the order parameter with respect to the inverse temperature. The estimate for the exponent $1/\nu$ is given in the panel by applying a simultaneous fitting attempt to a simple power law in the size range $L = 12 - 44$.

of the order parameter with respect to the inverse temperature [see Eq. (4)]. Their behavior was observed to be quite stable and consistent with the above estimation from the shift behavior. We tried here to vary again the ranges from $L = 8 - 44$ to $L = 28 - 44$. Depending on L_{min} the estimated effective exponents vary in the range $1/\nu = 1.445 - 1.415$. In Fig. 11 we illustrate such an estimation by a simultaneous fitting attempt in the range $L = 12 - 44$. As it can be seen from this figure the estimate is $1/\nu = 1.440(2)$. Therefore, from this FSS scheme one should conclude that $1/\nu = 1.430(10)$ and combining with the above shift behavior, we should regard $1/\nu = 1.440(10)$ a very decent proposal that is now in full agreement with the exponent value $1/\nu = 1.438$ obtained by satisfying hyperscaling, given the previous estimates for $\gamma/\nu = 1.864$ and $(1 - \beta)/\nu = 0.87$.

Finally we give an outline on the behavior of the order parameter at the estimated critical temperature. We computed the finite-size values of the order parameter at the temperature $T_c = 1.6835$ from the corresponding (sample-averaged) order-parameter curves. In Fig. 12 we apply a simple power-law estimation for the exponent ratio β/ν , using again the size range $L = 12 - 44$. This estimation gives a critical exponent ratio $\beta/\nu = 0.566(5)$ in excellent agreement with the value $\beta/\nu = 0.568$, which is obtained by satisfying hyperscaling, given the estimates $\gamma/\nu = 1.864$ and $(1 - \beta)/\nu = 0.87$. Furthermore, it should be noted that the total variation with the lattice-size range is very small, ranging from $\beta/\nu = 0.56(1)$ to $\beta/\nu = 0.57(2)$, as we vary the size range from $L = 8 - 44$ to $L = 24 - 44$.

Summarizing, our findings in this Section on the emerging, under bond randomness, second-order phase transition of the 3d random-bond BC model are the fol-

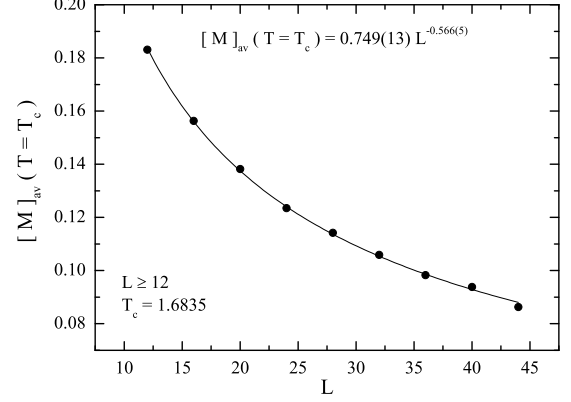


FIG. 12: FSS behavior of the order parameter at the estimated critical temperature. In the panel we show a simple power-law estimation of the exponent ratio β/ν .

lowing: (i) the proposed critical exponents provide a stable finite-size behavior, strongly supporting hyperscaling and (ii) the proposed value of the critical exponent $\gamma/\nu = 1.864(12)$ characterizes, in a very clear way, the expected distinctive strong-coupling fixed point, describing, according to the renormalization-group calculations, the emerging from the first-order regime second-order phase transition.

V. SUMMARY AND CONCLUSIONS

It is instructive at this point to attempt an overview on the effects of disorder for 3d ex-second- and ex-first-order phase transitions and compare our results with previous relevant research. Let us restrict ourselves to a presentation focused mainly on some of the papers discussed already in the text. These are the cases of the 3d RIM [17, 20, 22] and those of the ex-weak first-order phase transition of the 3d site-diluted $q = 3$ Potts model studied by Ballesteros *et al.* [32], and the case of the ex-strong first-order transition of the 3d bond-diluted $q = 4$ Potts model studied by Chatelain *et al.* [33]. In table I we display the critical exponents obtained in these papers together with the two concrete cases of the random-bond 3d BC Model. From this table one can see that, for the two cases studied here, the hyperscaling relation $(2\beta/\nu) + \gamma/\nu = d$ is well satisfied, and the best case is that of the ex-first-order transition that was also found to have a very robust FSS behavior. Furthermore, a straightforward comparison shows that, our ex-second-order case ($\Delta = 1$; $r = 1/3$) has a very similar behavior with that of Berche *et al.* [22] on the 3d bond-diluted Ising model with magnetic bond concentration $p = 0.7$. This is quite remarkable and, we may also point out that, our results are limited to lattice sizes up to $L = 44$, whereas sizes up to $L = 96$ have been simulated in that paper. Our

TABLE I: Summary of critical exponents for the 3d pure and disordered Ising (IM), q -states Potts (PM), and Blume-Capel (BCM) models, as obtained in Refs. [17, 20, 22, 32, 33, 64, 65] and the present paper.

Model	$1/\nu$	ν	γ/ν	$\eta = 2 - \gamma/\nu$	β/ν	$(2\beta/\nu) + \gamma/\nu$
Ex-second-order phase transition						
Pure IM [64]	1.586(3)	0.6304(13)	1.966(3)	0.034(3)	0.517(3)	3.00(9)
Pure IM [65]		0.63002(10)		0.03627(10)		
Site-diluted IM($p = 0.8$) ^a [17]	1.463(11)	0.6837(53)	1.963(5)	0.037(5)		
Site-diluted IM($p = 0.8$) ^a [20]		0.683(2)		0.036(1)		
Bond-diluted IM ($p = 0.7$) ^a [22]	1.520(20)	0.660(10)	1.965(10)	0.035(10)	0.515(5)	2.995(20)
Bond-diluted IM ($p = 0.55$) ^a [22]	1.460(20)	0.685(10)	1.977(10)	0.023(10)	0.513(5)	3.003(20)
Random-bond BCM ($\Delta = 1$; $r = 1/3$)	1.504(19)	0.665(17)	1.964(4)	0.036(4)	0.510(10)	2.984(24)
Ex-first-order phase transition						
Bond-diluted $q = 3$ PM [32]	1.449(10)	0.690(5)	1.922(4)	0.078(4)		
Random-bond BCM ($\Delta = 2.9$; $r = 1/3$)	1.440(10)	0.694(5)	1.864(12)	0.136(12)	0.566(5)	2.996(22)
Bond-diluted $q = 4$ PM [33]	1.330(25)	0.752(14)	1.500(14)	0.500(14)	0.645(24)	2.790(62)

^a1 - p denotes the concentration of impurities.

efforts indicate, in agreement with Berche *et al.* [22], that at these lattice sizes the system still crosses over to the universality class of the RIM, described by the second entry in table I [17]. Finally, we have deliberately placed our second case of study of the random-bond BC Model ($\Delta = 2.9$; $r = 1/3$) after the ex-weak- and before the ex-strong-first-order transitions of the 3d Potts model, since our results for the critical exponents appear to interpolate between these two cases.

In conclusion, the 3d random-bond BC model has been studied numerically in both its first- and second-order phase transition regimes by a comprehensive FSS analysis. As expected on general universality arguments the 3d random-bond BC model at the second-order regime ($\Delta = 1$) was found to be fully compatible with the 3d Ising universality class. However, the case studied here $[(\Delta, r) = (1, 1/3)]$ exhibits analogous crossover problems as the ones encountered in the case of the bond-diluted 3d Ising model with magnetic bond concentration $p = 0.7$ studied by Berche *et al.* [22]. For the case of ex-first-order regime at $\Delta = 2.9$, we have shown that the disorder strength $r = 1/3$ was strong enough to convert, without doubt, the original first-order transition to a genuine second-order one. For this case $[(\Delta, r) = (2.9, 1/3)]$ we have presented a detailed and convincing FSS scheme. The scenario adopted in this paper, and the proposed critical exponents obtained from a stable scaling behavior, are supporting strongly hyperscaling. In particular the value of the critical exponent $\gamma/\nu = 1.864(12)$ is robust and characterizes, in a very clear way, the expected distinctive strong-coupling fixed point, describing, according to the renormalization-group calculations, the emerging from the first-order regime second-order phase transition. The present results point out, as in the case of the 2d random-bond BC model, the existence of a strong violation of universality principle of critical phenomena, since the two second-order transitions between

the same ferromagnetic and paramagnetic phases have different sets of critical exponents. In the 2d random-bond BC model the difference in the exponents was revealed in the thermal exponent ν and an extensive but weak universality was found corresponding to the fact that the two emerging transitions have the same magnetic exponent ratios (β/ν and γ/ν) [11]. However, for the 3d random-bond BC model no such weak universality is supported. The observed strong violation of universality is now revealed mainly, but not exclusively, in the fact that the corresponding emerging transitions have different magnetic exponent ratios, as seen from the values of γ/ν of table I.

The proposal for the possible new universality class in the 3d random BC model in the ex-first-order regime is an interesting finding supported also by the early renormalization-group calculations [4, 10], as mentioned already in the introduction. It is also a surprising result since the two transitions are between the same ferromagnetic and paramagnetic phases. However, having in mind that the 3d RIM suffers rather slowly decaying scaling corrections [17, 20, 22], one can never be confident for the asymptotic behavior at the present system sizes. In view of the above comments, and the earlier discussion of our fitting attempts for the susceptibility maxima, a confident resolution of this situation may require lattice sizes of the order of at least $L = 240$. Further investigations, for instance considering the behavior for different values of the crystal-field coupling Δ , suitably chosen in the ex-first-order regime, may be very useful to this direction. In a more advanced level one may try to obtain further convincing evidence by comparing multifractal spectra for correlations functions [60, 61] for the ex-second- and ex-first-order transitions. These lines of research demand further computational efforts and more sophisticated MC and FSS schemes, but as pointed out in subsection II B, may yield more precise and additional useful information

concerning the properties of disorder averages [18].

Acknowledgments

The authors are grateful to V. Martín-Mayor for a critical reading of the manuscript. This work was supported

by the special Account for Research of the University of Athens (code: 11112). N.G. Fytas has been partly supported by MICINN, Spain, through a research contract No. FIS2009-12648-C03.

-
- [1] A.B. Harris, J. Phys. C **7**, 1671 (1974).
 - [2] A.N. Berker, Phys. Rev. B **42**, 8640 (1990).
 - [3] M. Aizenman and J. Wehr, Phys. Rev. Lett. **62**, 2503 (1989); **64**, 1311(E) (1990).
 - [4] K. Hui and A.N. Berker, Phys. Rev. Lett. **62**, 2507 (1989); **63**, 2433(E) (1989).
 - [5] A.N. Berker, Physica A **194**, 72 (1993).
 - [6] J. Cardy and J.L. Jacobsen, Phys. Rev. Lett. **79**, 4063 (1997); J.L. Jacobsen and J. Cardy, Nucl. Phys. B **515**, 701 (1998); J. Cardy, Physica A **263**, 215 (1998).
 - [7] L.A. Fernández, A. Gordillo-Guerrero, V. Martín-Mayor, and J.J. Ruiz-Lorenzo, arXiv:1205.0247.
 - [8] R.L. Greenblatt, M. Aizenman and J.L. Lebowitz, Phys. Rev. Lett. **103**, 197201 (2009); Physica A **389**, 2902 (2010).
 - [9] S. Chen, A.M. Ferrenberg, and D.P. Landau, Phys. Rev. Lett. **69**, 1213 (1992).
 - [10] A. Falicov and A.N. Berker, Phys. Rev. Lett. **76**, 4380 (1996).
 - [11] A. Malakis, A.N. Berker, I.A. Hadjiagapiou, and N.G. Fytas, Phys. Rev. E **79**, 011125 (2009); A. Malakis, A.N. Berker, I.A. Hadjiagapiou, N.G. Fytas, and T. Papakonstantinou, *ibid.* **81**, 041113 (2010).
 - [12] F. Wang and D.P. Landau, Phys. Rev. Lett. **86**, 2050 (2001); Phys. Rev. E **64**, 056101 (2001).
 - [13] D.P. Landau, Phys. Rev. B **22**, 2450 (1980).
 - [14] D. Chowdhury and D. Stauffer, J. Stat. Phys. **44**, 203 (1986).
 - [15] H.-O. Heuer, Europhys. Lett. **12**, 551 (1990); Phys. Rev. B **42**, 6476 (1990); J. Phys. A **26**, L333 (1993).
 - [16] M. Hennecke, Phys. Rev. B **48**, 6271 (1993).
 - [17] H.G. Ballesteros, L.A. Fernández, V. Martín-Mayor, A. Muñoz Sudupe, G. Parisi, and J.J. Ruiz-Lorenzo, Phys. Rev. B **58**, 2740 (1998).
 - [18] S. Wiseman and E. Domany, Phys. Rev. Lett. **81**, 22 (1998); Phys. Rev. E **58**, 2938 (1998).
 - [19] P. Calabrese, V. Martín-Mayor, A. Pelissetto, and E. Vicari, Phys. Rev. E **68**, 036136 (2003).
 - [20] M. Hasenbusch, F. Parisen Toldin, A. Pelissetto, and E. Vicari, J. Stat. Mech.: Theory Exp. (2007) P02016.
 - [21] P.E. Berche, C. Chatelain, B. Berche, and W. Janke, Comp. Phys. Comm. **147**, 427 (2002).
 - [22] P.E. Berche, C. Chatelain, B. Berche, and W. Janke, Eur. Phys. J. B **38**, 463 (2004).
 - [23] D. Ivaneyko, J. Ilnytskyi, B. Berche, and Yu. Holovatch, Cond. Matt. Phys. **8**, 149 (2005).
 - [24] N.G. Fytas and P.E. Theodorakis, Phys. Rev. E **82**, 062101 (2010).
 - [25] M. Hasenbusch, F. Parisen Toldin, A. Pelissetto, and E. Vicari, Phys. Rev. B **76**, 094402 (2007).
 - [26] R. Folk, Y. Holovatch, and T. Yavorskii, Phys. Rev. B **61**, 15114 (2000).
 - [27] D.V. Pakhnin and A.I. Sokolov, Phys. Rev. B **61**, 15130 (2000).
 - [28] A. Pelissetto and E. Vicari, Phys. Rev. B **62**, 6393 (2000).
 - [29] K.E. Newman and E.K. Riedel, Phys. Rev. B **25**, 264 (1982).
 - [30] G. Jug, Phys. Rev. B **27**, 609 (1983).
 - [31] I.O. Mayer, J. Phys. A **22**, 2815 (1989).
 - [32] H.G. Ballesteros, L.A. Fernández, V. Martín-Mayor, A. Muñoz Sudupe, G. Parisi, and J.J. Ruiz-Lorenzo, Phys. Rev. B **61**, 3215 (2000).
 - [33] C. Chatelain, B. Berche, W. Janke, and P.E. Berche, Phys. Rev. E **64**, 036120 (2001); Nucl. Phys. B **719**, 725 (2005).
 - [34] I. Puha and H.T. Diep, J. Magn. Magn. Mater. **224**, 85 (2001).
 - [35] O.D.R. Salmon and J.R. Tapia, J. Phys. A **43**, 125003 (2010).
 - [36] X.T. Wu, Phys. Rev. E **82**, 010101 (2010).
 - [37] D.A. Dias and J.A. Plascak, Phys. Lett. A **375**, 2089 (2011).
 - [38] M. Blume, Phys. Rev. **141**, 517 (1966).
 - [39] H.W. Capel, Physica (Utr.) **32**, 966 (1966); **33**, 295 (1967); **37**, 423 (1967).
 - [40] D.P. Landau, Phys. Rev. Lett. **28**, 449 (1972); A.N. Berker and M. Wortis, Phys. Rev. B **14**, 4946 (1976); M. Kaufman, R.B. Griffiths, J.M. Yeomans and M. Fisher, *ibid.* **23**, 3448 (1981); W. Selke and J. Yeomans, J. Phys. A **16**, 2789 (1983); D.P. Landau and R.H. Swendsen, Phys. Rev. B **33**, 7700 (1986); J.C. Xavier, F.C. Alcaraz, D. Pena Lara, and J.A. Plascak, *ibid.* **57**, 11575 (1998).
 - [41] M.J. Stephen and J.L. McCole, Phys. Rev. Lett. **44**, 89 (1973); T.S. Chang, G.F. Tuthill, and H.E. Stanley, Phys. Rev. B **9**, 4482 (1974); G.F. Tuthill, J.F. Nicoll, and H.E. Stanley, *ibid.* **11**, 4579 (1975); F.J. Wegner, Phys. Lett. **54A**, 1 (1975).
 - [42] P.F. Fox and A.J. Guttmann, J. Phys. C **6**, 913 (1973); T.W. Burkhardt and R.H. Swendsen, Phys. Rev. B **13**, 3071 (1976); W.J. Camp and J.P. Van Dyke, *ibid.* **11**, 2579 (1975); D.M. Saul, M. Wortis, and D. Stauffer, *ibid.* **9**, 4964 (1974).
 - [43] P. Nightingale, J. Appl. Phys. **53**, 7927 (1982).
 - [44] P.D. Beale, Phys. Rev. B **33**, 1717 (1986).
 - [45] A.K. Jain and D.P. Landau, Phys. Rev. B **22**, 445 (1980).
 - [46] D.P. Landau and R.H. Swendsen, Phys. Rev. Lett. **46**, 1437 (1981).
 - [47] C.M. Care, J. Phys. A **26**, 1481 (1993).
 - [48] M. Deserno, Phys. Rev. E **56**, 5204 (1997).
 - [49] H.W.J. Blöte, E. Luijten, and J.R. Heringa, J. Phys. A **28**, 6289 (1995).
 - [50] Y. Deng and H.W.J. Blöte, Phys. Rev. E **70**, 046111 (2004).
 - [51] C.J. Silva, A.A. Caparica, and J.A. Plascak, Phys. Rev.

- E **73**, 036702 (2006).
- [52] N. Metropolis, A.W. Rosenbluth, M.N. Rosenbluth, A.H. Teller, and E. Teller, J. Chem. Phys. **21**, 1087 (1953).
 - [53] R.H. Swendsen and J.S. Wang, Phys. Rev. Lett. **58**, 86 (1987); U. Wolff, *ibid.* **62**, 361 (1989).
 - [54] M.E.J Newman and G.T. Barkema, *Monte Carlo Methods in Statistical Physics* (Clarendon, Oxford, 1999).
 - [55] D.P. Landau and K. Binder, *Monte Carlo Simulations in Statistical Physics* (Cambridge University Press, Cambridge, 2000).
 - [56] E. Bittner and W. Janke, arXiv: 1107.5640v1.
 - [57] A. Malakis, G. Gulpinar, Y. Karaaslan, T. Papakonstantinou, and G. Aslan, Phys. Rev. E **85**, 031146 (2012).
 - [58] D.S. Fisher, Phys. Rev. B **51**, 6411 (1995).
 - [59] J.T. Chayes, L. Chayes, D.S. Fisher, and T. Spencer, Phys. Rev. Lett. **57**, 299 (1986); Comm. Math. Phys. **120**, 501 (1989).
 - [60] A.W.W. Ludwig, Nucl. Phys. B **330**, 639 (1990).
 - [61] C. Monthus, B. Berche, and C. Chatelain, J. Stat. Mech.: Theory Exp. (2009) P12002.
 - [62] A.M. Ferrenberg and D.P. Landau, Phys. Rev. B **44**, 5081 (1991).
 - [63] K. Binder, Z. Phys. B **43**, 119 (1981).
 - [64] R. Guida and J. Zinn-Justin, J. Phys. A **31**, 8103 (1998).
 - [65] M. Hasenbusch, Phys. Rev. B **82**, 174433 (2010).
 - [66] M. Campostrini, A. Pelissetto, P. Rossi, and E. Vicari, Phys. Rev. E **65**, 066127 (2002).
 - [67] P. Butera and M. Comi, Phys. Rev. B **65**, 144431 (2002); *ibid.* **72**, 014442 (2005).